



A multiparametric analysis based on DCE-MRI to improve the accuracy of parotid tumor discrimination

Zhifeng Xu¹ · Shaoyan Zheng² · Aizhen Pan¹ · Xiaofang Cheng³ · Mingyong Gao¹

Received: 15 April 2019 / Accepted: 16 July 2019 / Published online: 1 August 2019
© Springer-Verlag GmbH Germany, part of Springer Nature 2019

Abstract

Background Recently, semiquantitative time-intensity curve (TIC) analysis based on DCE-MRI and apparent diffusion coefficient (ADC) value-based diffusion-weighted imaging (DWI) were used to improve the diagnostic efficiency when diagnosing parotid tumors (PTs). However, quantitative DCE-MRI biomarkers have not been emphasized previously.

Purpose To explore the diagnostic efficiency of perfusion parameters alone or in combination based on quantitative DCE-MRI and DWI in the differential diagnosis of PTs.

Methods In total, 112 patients with parotid masses were prospectively recruited in our hospital from August 2013 to March 2017. All patients were evaluated with DCE-MRI and DWI before surgery. TIC and quantitative parameters based on DCE MRI and ADCs were analyzed. Receiver operating characteristic analysis and linear discriminant analysis (LDA) was used to determine their diagnostic performance.

Results In total, 87% (27/31) of pleomorphic adenoma (PA) showed type A TIC, 74% (65/88) of Warthin's tumors showed type B TIC, and 95% (19/20) of malignant tumors showed TIC type C. Pearson χ^2 test showed a significant difference between TIC patterns in benign and malignant tumors ($\chi^2 = 38.78$, $p < 0.001$). ROC analysis revealed that ADC achieved the best diagnostic performance for distinguishing PA and Warthin's tumor from others, with area under the curve (AUC) values of 0.945 and 0.925 ($p < 0.01$), respectively. Furthermore, the TIC type was the only useful biomarker for distinguishing malignant from benign PTs, with an AUC of 0.846 ($p < 0.01$). Concerning the accuracy of the combined application of multiple parameters of DCE-MRI and ADC values, a combination of TIC pattern and extracellular volume ratio (Ve) provided the best results among five protocols, producing the highest accuracy of 0.75, followed by the combined use of the TIC pattern and ADC (accuracy was 0.70).

Conclusion TIC pattern in combination with the Ve biomarker based on DCE-MRI could achieve optimal diagnostic accuracy in the differential diagnosis of PTs.

Keywords Parotid tumor · DCE-MRI · Diffusion-weighted imaging (DWI) · Apparent diffusion coefficients (ADC) · Linear discriminant analysis (LDA)

This article is part of the Topical Collection on Oncology—Head and Neck

✉ Zhifeng Xu
xuzf83@126.com

¹ Department of Radiology, The First People's Hospital of Foshan, Foshan, Guangdong, China

² Department of MR, Shantou Central Hospital, Shantou, Guangdong, China

³ Department of Radiology, Affiliated Brain Hospital of Guangzhou Medical University (Guangzhou Hui'ai Hospital), Guangzhou, People's Republic of China

Introduction

The characterization of parotid tumors is important for pre-operative treatment planning. Postcontrast-computed tomography and perfusion-computed tomography improved the differential diagnosis of parotid tumors [1, 2], but these tumors are eradicated with radiation exposure and low soft tissue resolution. Conventional magnetic resonance imaging (MRI) is valuable for identifying the tumor location, morphology, extension, relationship with the facial nerve, and inner structure [3]. However, it is not always possible to establish the diagnosis with these parameters alone. Dynamic contrast-

enhanced (DCE) MRI is used to track the path of an exogenous, paramagnetic contrast agent through tissues and has emerged as a powerful tool in the characterization of tumor hemodynamics [4]. In recent years, semiquantitative time-intensity curve (TIC) analysis based on DCE-MRI was used to improve the diagnostic efficiency of parotid tumors [4, 5]. Previous studies [2, 4–6] showed that time to peak (TTP) was closely related with microvessel count and wash out ratio (WR) and accurately reflects the stromal cellularity grade. However, reports have indicated significant overlap of the TIC of benign and malignant tumors. Recently, studies have shown that analysis using TICs and apparent diffusion coefficients (ADCs) could be potential tools for the differentiation of tumor types [5, 7]. The single use of these MRI techniques has yielded acceptable results, but the diagnostic efficacy was not high. As we know, except for TIC, many perfusion biomarkers, such as K_{trans} (volume transfer constant between blood plasma and extracellular extravascular space [EES]), V_e (EES fractional volume), and K_{ep} (flux rate constant between the EES and plasma), are also available for the quantitative analysis of DCE-MRI and are well correlated with histological findings. However, previous research about these biomarkers of quantitative DCE-MRI in parotid tumor diagnosis is rare, and the diagnostic value of these biomarkers is unclear. The main objective of this study was to explore methods to improve the diagnostic efficiency of perfusion parameters (TIC, K_{trans} , K_{ep} , and V_e) alone or in combination when diagnosing parotid tumors based on quantitative DCE-MRI.

Methods and materials

Patients

This prospective study was approved by the institutional review board (Ethics committee of Foshan First People's Hospital and Ethics committee of Shantou Central Hospital) and performed between August 2013 and March 2017. Informed consent was obtained from all individual participants included in the study. DCE-MRI and ADC were prospectively performed on consecutive patients with clinically suspected primary parotid tumors. Exclusion criteria were as follows: (1) Presence of hemangioma, lymphangioma, lipomyoma, or cyst was reliably diagnosed by clinical and radiological methods. (2) Lesions after treatment and recurrent lesions were both removed. (3) Patient contraindications (such as claustrophobia or many fixed dentures). (4) Patients who were not suitable for MRI examination (patients with head and neck disease requiring postoperative stent placement). All patients underwent surgery, and histopathologic diagnosis was based on findings in specimens obtained by surgical resection.

Finally, 112 patients with 148 parotid masses confirmed by surgical pathology were included.

Routine MR imaging and DCE-MRI

MR imaging was performed on a 3.0 T superconducting MR imaging system (Siemens MAGNETOM Verio 3.0 T, Germany) with head and neck array coils. Routine MR sequences included tra-T1W (TR/TE, 550 ms/8.7 ms), tra-T2W (TR/TE, 5500 ms/95 ms), and cor-T2W-tirm (TR/TE/TI, 3000 ms/39 ms/220 ms). DCE-MRI was performed with a T1-weighted 3D spoiled gradient echo sequence (3D volume interpolated body examination, 3D-vibe; TR/TE, 5.08 ms/1.74 ms; flip angle 15°). The contrast agent Gd-DTPA (Magnevist, Schering, China) was injected after fourth dynamic sequence acquisition at a rate of 2.0 ml/s via the right antecubital vein. The contrast agent was administered at a concentration of 0.2 mmol/kg body weight. After contrast agent injection, a 20-mL saline flush at the same injection rate was immediately performed. In total, 35 dynamic sequence acquisitions with 20 dynamic images per sequence were performed with a total scan time of 5 min and 20 s. Prior to dynamic image acquisitions, pre-contrast images were obtained with two flip angles of 2° and 15° for T1 mapping.

Diffusion-weighted MR imaging

Diffusion-weighted MR imaging was performed by using a multislice echo-planar (EPI) single-shot spin-echo sequence, in the transverse plane (TR/TE = 3200/118 ms, FOV = 20–25 cm, matrix = 128 × 128, section thickness = 5 mm and interslice gap = 2 mm). Three diffusion gradients were applied sequentially in the x , y , and z directions with b values of 0, 500, and 1000 s/mm². The acquisition time was 48 s. The ADC maps were automatically generated.

Image analysis

Image analysis was performed by 1 radiologist (S.S.), who is an expert in MR imaging, has 18 years of experience, and was blinded to the clinical diagnosis. The sequential dynamic MR images were transferred in a Digital Imaging and Communications in Medicine (DICOM) format onto a postprocessing workstation and were subsequently analyzed by using ImageJ (NIH) and Mathematica (Wolfram Research) software. To ascertain the accuracy of TIC and perfusion biomarkers analysis, ROIs were drawn to avoid the vascular and cystic parts of the tumors. When contrast enhancement was heterogeneous, the signal intensities of multiple areas were measured. In addition, the area with maximal enhancement was selected for ROI location, and the corresponding ROIs for ADC measurements were drawn. Semiquantitative analysis of DCE-MRI was based on TIC. Each of the obtained TICs

was automatically classified based on the increment ratio, the time to peak enhancement (T_{peak}), and the washout ratio (WR) into four (A–D) types according to the process described by Takashi Nakamura [8]. Quantitative analysis of DCE-MRI was based on the automatic generalized mode. In this model, the contrast agent movement between tissue compartments is related to three physiologically based parameters: K_{trans}, K_{ep}, and V_e.

Statistical analysis and linear discriminant analysis

All statistical analyses were performed by using the Statistical Package for Social Sciences, Version 17.0 (SPSS 17.0). Pearson χ^2 was used for comparison of TIC types among different histological types of parotid gland tumors. DCE-MRI quantitative parameters (K_{trans}, K_{ep}, and V_e) were assessed among different histologic types of parotid gland tumors based on the Kruskal–Wallis *H* test and Mann–Whitney *U* test. $p < 0.05$ was considered statistically significant. TIC types and threshold values for various parameters were determined by receiver operating characteristic curve (ROC)-based tests. Sensitivity, specificity, accuracy, and positive and negative predictive values for DCE-MRI in diagnosing malignant parotid tumors were calculated. Linear discriminant analysis (LDA) was used to evaluate the separability of different histological types of the parotid gland tumors of the testing set using TIC types, ADC, and perfusion parameters (K_{trans}, K_{ep} and V_e). Half of the tumors in each group tumor were selected as the training set, and the remaining half cases were used as the testing set. In total, 100 operations were performed randomly. The accuracy of different composite

indexes for different histological types of tumor identify was evaluated.

Results

Clinical and histopathologic results

A total of 112 patients (62 men and 50 women) qualified for the final analysis of the study. The patients' age ranged between 16 and 84 years (mean, 58 years). The final pathological diagnosis of parotid tumors was as follows: PAs ($n = 31$), Warthin's tumor ($n = 52$), malignant tumors ($n = 20$) (including squamous cell carcinoma ($n = 7$); acinic cell carcinoma ($n = 3$); lymphoepithelial carcinoma ($n = 3$); adenoid cystic carcinoma ($n = 2$); lymphoma ($n = 1$); mucoepidermoid carcinoma ($n = 2$); duct carcinoma ($n = 1$); basal cell adenocarcinoma ($n = 1$)), and other benign tumors ($n = 9$) (including basal cell adenoma ($n = 5$); oncocytic adenoma ($n = 1$); monomorphic adenoma ($n = 2$); facial nerve schwannoma ($n = 1$)).

DCE-MRI and ADC analysis

TIC types of different histopathologic tumors are shown in Fig. 1a. Type D TIC was not present in this study. The great majority of PAs and Warthin's tumor exhibited type A TIC (Fig. 2) and type B TIC (Fig. 3), respectively, accounting for 87% (27/31) and 74% (65/88), respectively. However, 95% (19/20) malignant tumors exhibited type C TIC (Fig. 4). Type A TIC was absent in Warthin's tumor and malignant tumors, whereas type B TIC was absent in PAs. Pearson χ^2 test showed a significant difference in TIC patterns between

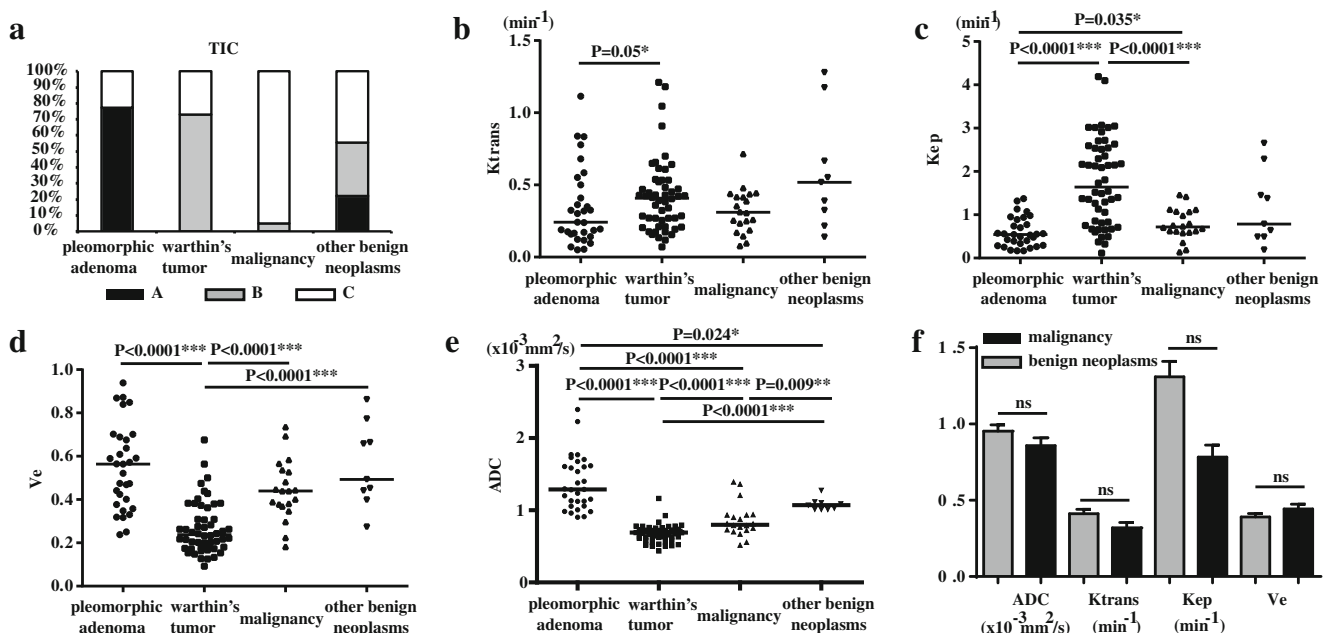


Fig. 1 Characterization of TIC types, multiparametric biomarkers, and ADC values of parotid tumors in different histopathologic groups

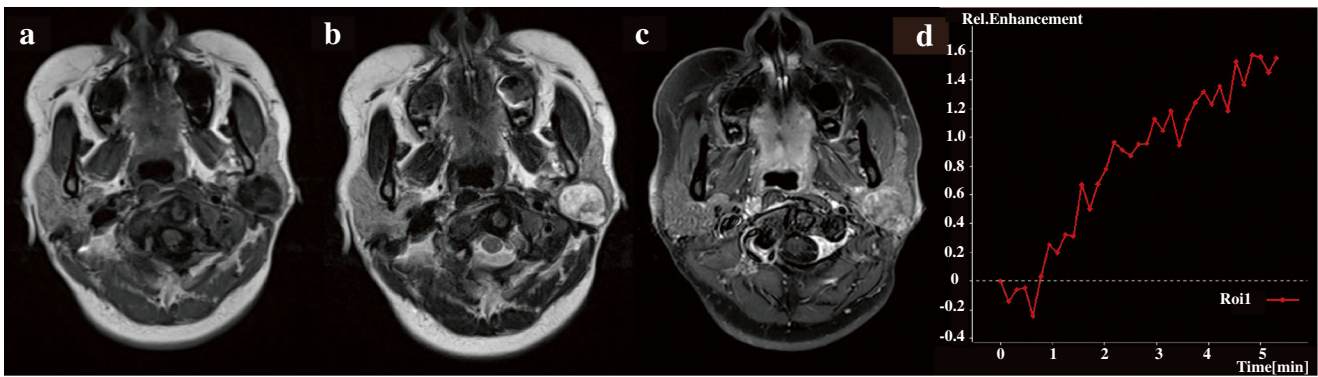


Fig. 2 PA in the right parotid. **a** Axial T2WI showing mixed hyperdense and isodense nodules. **b** Axial T1WI showing isodense nodules. **c** DCE-T1WI showing nonhomogeneous enhanced nodules. **d** Type A TIC

benign and malignant tumors ($\chi^2 = 38.78, p < 0.001$). Type A TIC and type B TIC indicated benign lesions, whereas type C TIC strongly indicated malignancy.

Mean quantitative parameter values (Ktrans, Kep, and Ve of DCE-MRI and ADC) of different histopathologic parotid tumors are shown in Table 1. The mean Ktrans of PAs was lowest with slightly different from that of Warthin’s tumor ($p = 0.05$) (Fig. 1b). The mean Kep of PAs and Warthin’s tumor was lowest and highest, respectively. In addition, the mean Kep was significantly different ($p < 0.01$) between each other in malignant tumors, PAs, and Warthin’s tumor (Fig. 1c). The mean Ve of Warthin’s tumor was lowest ($p < 0.01$) (Fig. 1d). The mean ADC of PAs was highest, followed by other benign tumors, malignant tumors, and Warthin’s tumor, and was significantly different between any two tumor types (Fig. 1e). Additionally, large overlap was observed in Ktrans and Kep among all different histopathologic parotid tumors.

Diagnostic efficiency of multiple parameters of DCE-MRI and ADC values

ROC curves (Fig. 5) showed that ADC was the best parameter for distinguishing PA from others, with an AUC of 0.945 ($p < 0.01$), followed by TIC types, with an AUC of 0.81

($p < 0.01$). In addition, ADC was also the best parameter for distinguishing Warthin’s tumor from others with an AUC of 0.925 ($p < 0.01$), followed by VE and Kep, with AUC values of 0.882 and 0.812, respectively ($p < 0.01$). Furthermore, TIC type was the only useful biomarker for distinguishing malignant from benign lesions with an AUC of 0.846 ($p < 0.01$). Compared with the accuracy of the combined application of multiple parameters of DCE-MRI and ADC values for differential diagnosis, TIC-Ve was the best biomarker for distinguishing parotid tumors, demonstrating the highest accuracy of 0.75, which was followed by TIC-ADC, with an accuracy of 0.70 ($p = 0.034$) (Fig. 6).

Discussion

The main finding of our study is that the combination of TIC pattern and Ve provided the best results among the five protocols, producing the highest accuracy of 0.75, which was followed by the combination of TIC pattern and ADC, yielding an accuracy of 0.70. Although some studies indicated that the combined use of contrast-enhanced (DCE) MRI and diffusion-weighted imaging (DWI) achieved the optimal diagnostic performance for the diagnosis of parotid tumors [6, 9,

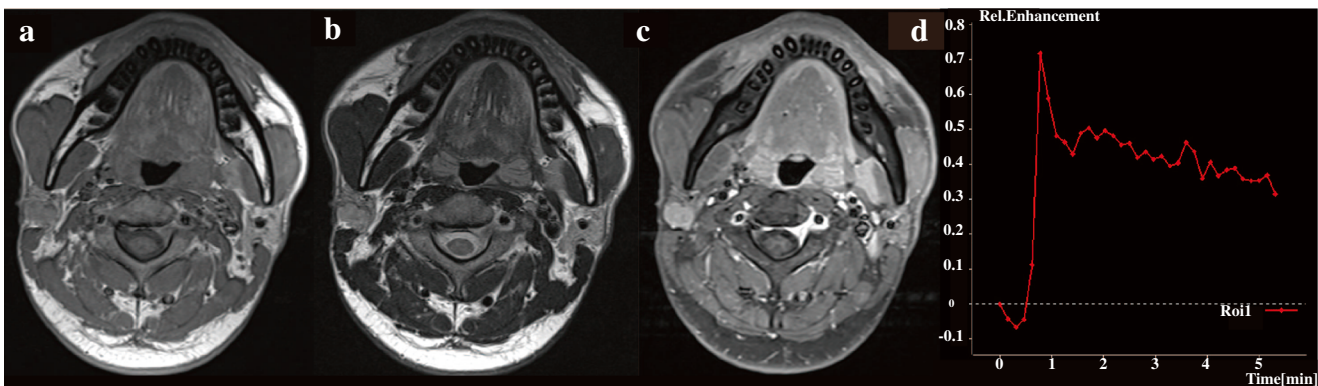


Fig. 3 Warthin’s tumor in the left parotid gland. **a** Axial T2WI the nodule showing slightly hyperintense and isointense signals. **b** Axial T1WI tumor showing an isointense signal. **c** Nodule showing slight homogeneous enhancement on DCE T1WI. **d** Type B TIC

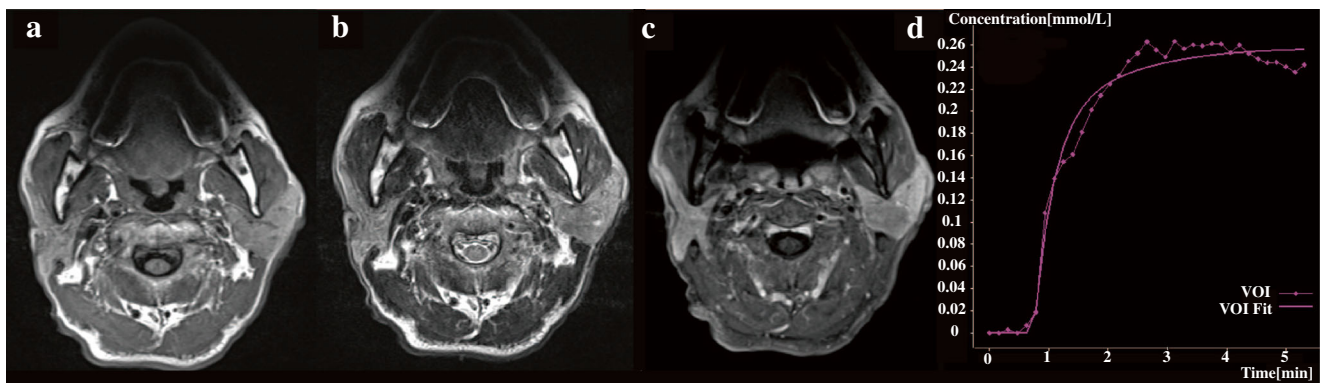


Fig. 4 Lymphoepithelial carcinoma in the right parotid gland. **a** Axial T2WI of nodule showing slight hyperdense and isodense areas. **b** Axial T1WI showing isodense nodules. **c** DCE-T1WI showing a slight homogeneous enhancement. **d** Type C TIC

10], significant overlaps between the ADC maps of benign and malignant salivary gland tumors have also been reported [4, 6, 11–13]. In addition, certain TIC pattern (type C) strategies yield high sensitivity but relatively low specificity. In our study, we compared the diagnostic efficiency of the use of perfusion parameters (TIC types, K_{trans} , K_{ep} and V_e) alone or in combination based on quantitative DCE-MRI and DWI in differential diagnosis of parotid tumors, demonstrating that the combined use of semiquantitative (TIC types) and quantitative techniques based on DCE-MRI was significantly better than the combination of TIC pattern and ADC or other perfusion parameters.

To our knowledge, TIC patterns are different for benign and malignant tumors. Specifically, the signal intensity curve grows rapidly in the first phase after contrast injection and decreases gradually in the next phase, whereas TIC curves of benign tumors exhibit an increasing trend [14]. Our result is consistent with this theory, indicating that TIC type is the only useful biomarker for distinguishing malignant from benign parotid tumors. In addition, ADC values calculated from DWI provided additional quantitative information through Brownian motion of water molecules in tissues. Previous reports revealed that the predictive value significantly improved with the addition of ADC values when evaluating patients with type B or C tumors [9, 10, 12, 15]. Likewise, our study confirmed that ADC achieved the best diagnostic performance for distinguishing PAs and Warthin's tumor from others, with area under the curve (AUC) values of 0.945 ($p < 0.01$) and 0.925 ($p < 0.01$), respectively. The mean ADC values of malignant tumors were significantly lower

than PAs and significantly higher than Warthin's tumor. Our result was consistent with that of Yabuuchi's study. They attributed this result to different tissue cellularity among PAs, Warthin's tumor, and malignant tumors [15]. However, given the lymphoid accumulation of Warthin's tumor resembling lymphoma demonstrated by Habermann et al [13], the provided ADC value for Warthin's tumor overlapped with examined malignant lesions, proving a limited value of ADC-based tumor differentiation focused on Warthin's tumor in an individual case. Despite limited temporal resolution of DCE-MRI, however, the spatial resolution is higher, which makes DCE more accurate in mixed lesions. A previous study validated that the T_{peak} and WR derived from TICs at DCE MR correlate well with histopathologic findings. Specifically, T_{peak} correlated closely with microvessel count, and the washout ratio (WR) accurately reflected the stromal cellularity grade [16]. Based on the article by Yabuuchi [15], we chose a T_{peak} of 120 s and a WR of 30% and categorized time-intensity curve (TIC) patterns into 4 types. Consistent with previous studies [9, 12, 14], our series revealed that 87% (27/31) of PAs presented type A TIC, and 74% (65/88) of Warthin's tumor presented type B TIC. Type C curves predominated malignant lesions with the exception of one single case. TIC types A, B, and D indicated benignancy, and type C indicated malignancy; these results yielded high sensitivity but relatively low specificity when malignancy was considered a positive result due to the inclusion of benign cases.

Multiparametric analysis is an optimal approach to improve differentiation of parotid tumors. In this study, we analyzed quantitative parameters values (including K_{trans} , K_{ep} , and V_e) among

Table 1 Quantitative DCE-MRI parameters and ADC values of different histopathologic parotid tumors

	K_{trans} (min^{-1})	K_{ep} (min^{-1})	V_e	ADC ($\times 10^{-3}$ mm^2/s)
Malignant tumors	0.327 ± 0.030	0.784 ± 0.064	0.445 ± 0.025	0.858 ± 0.253
Pleomorphic adenomas	0.217 ± 0.036	0.567 ± 0.048	0.549 ± 0.278	1.367 ± 0.376
Warthin's tumor	0.464 ± 0.036	1.806 ± 0.111	0.272 ± 0.013	0.669 ± 0.126
Other benign tumors	0.663 ± 0.092	1.358 ± 0.205	0.528 ± 0.431	1.036 ± 0.168

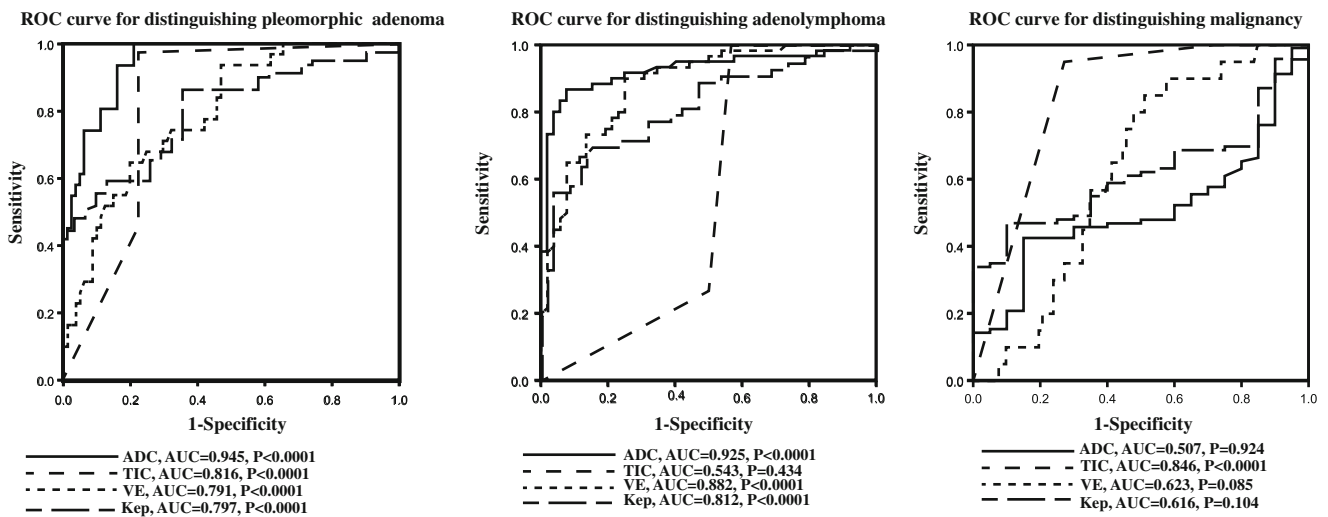


Fig. 5 ROC curves of multiple parameters of DCE-MRI and ADC values for differential diagnosis

different pathologic types of parotid tumors and compared the diagnostic ability among different protocols. The results showed that the mean Kep values of Warthin’s tumor were significantly higher than those of PAs and malignant tumors, whereas the mean Ve value of Warthin’s tumor was significantly lower than that of malignant tumors and PAs. One possible explanation for the high Kep and low Ve value for Warthin’s tumor may be related to the limited extracellular and extravascular space of these tumors [17]. The mean Ktrans of PAs was slightly lower than that of Warthin’s tumor and malignant tumors; however, the difference did not reach statistical significance. Concerning the diagnostic accuracy of the perfusion parameters (TIC, Ktrans, Kep, and Ve) alone or combined with quantitative parameters and DWI in the differential diagnosis of parotid tumors, we found that the combination of TIC pattern and Ve gave the best results among the five protocols, achieving the highest accuracy

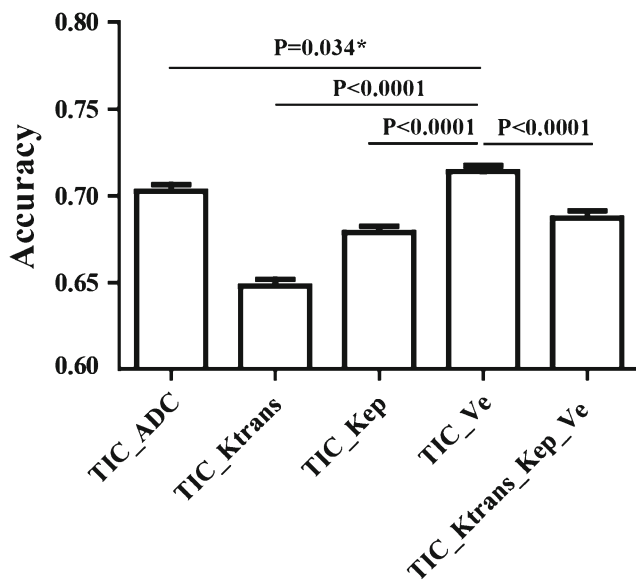


Fig. 6 The accuracy of the combined application of multiple parameters of DCE-MRI and ADC values for diagnosis

of 0.75, followed by the combined use of the TIC pattern and ADC. In our study, Ve values were superior to ADC values. Given that the overlap of ADCs between Warthin’s tumor and malignant tumors has been previously revealed, we postulate that it may be attributed to the fact that there is less overlap between Ve values for parotid tumors. Furthermore, by performing a longitudinal study investigating salivary DCE-MRI changes, Ger et al. [18] demonstrated that Ve was the only parameter that had a consistently significant longitudinal difference, suggesting that Ve may be a more sensitive indicator when compared with other perfusion parameters and ADCs.

There were several limitations in the current study. First, the sample size, especially for the malignant group included in this study, was relatively small, which may result in an over-estimation of the diagnostic accuracy. Second, potential bias within the manual definition ROI is inevitable, which might increase the variability of quantitative measurements. Finally, ADC was generally deemed to be an imaging biomarker that was inversely correlated with tumor cellularity, but no correlation was observed between Ve and ADC in glioblastoma and breast cancer. Therefore, the actual physiological meaning of Ve needs to be clarified.

Conclusion

Our results showed that ADC was the best parameter for distinguishing PAs and Warthin’s tumor from others, followed by TIC type ($p < 0.01$). However, TIC type is the only useful biomarker for distinguishing malignant from benign lesions, with an AUC of 0.846 ($p < 0.01$). Compared with the accuracy of combined application of multiple parameters of DCE-MRI and ADC values for differential diagnosis, the combination of TIC pattern and Ve biomarker based on the DCE-MRI can achieve optimal diagnostic accuracy in the differential diagnosis of parotid tumors.

Acknowledgments The authors thank Jin-Yabin from the First People's Hospital of Foshan for the help in figure editing.

Compliance with ethical standards

Conflict of interest The authors declare that they have no conflict of interest.

Ethical approval This prospective study was approved by the institutional review board (Ethics committee of Foshan First People's Hospital and Ethics Committee of Shantou Central Hospital) and performed between August 2013 and March 2017. Informed consent was obtained from all individual participants included in the study.

References

- Xu ZF, Yong F, Yu T, Chen YY, Gao Q, Zhou T, et al. Different histological subtypes of parotid gland tumors: CT findings and diagnostic strategy[J]. *World J Radiol.* 2013;5(8):313–20. <https://doi.org/10.4329/wjr.v5.i8.313>.
- Xu Z, Rong F, Yu T, Chen YY, Gao Q, Zhou T, et al. Pleomorphic adenoma versus Warthin tumor of the parotid gland: diagnostic value of CT perfusion imaging and its pathologic explanation:CT perfusion of pleomorphic adenoma versus Warthin[J]. *J Tumor.* 2016;4(2):419–25. <https://doi.org/10.17554/j.issn.1819-6187.2016.04.74>.
- Matsusue E, Fujihara Y, Matsuda E, Tokuyasu Y, Nakamoto S, Nakamura K, et al. Vanishing Parotid Tumors on MR Imaging[J]. *Yonago Acta Med.* 2018;61(1):33–9 eCollection 2018 Mar. 2018;61:033–039.
- Eida S, Sumi M, Nakamura T. Multiparametric magnetic resonance imaging for the differentiation between benign and malignant salivary gland tumors[J]. *JMRI.* 2010;31:673–9. <https://doi.org/10.1002/jmri.22091>.
- Sumi M, Van Cauteren M, Sumi T, Obara M, Ichikawa Y, Nakamura T. Salivary gland tumors: use of intravoxel incoherent motion MR imaging for assessment of diffusion and perfusion for the differentiation of benign from malignant tumors[J]. *Radiology.* 2012;263(3):770–7. <https://doi.org/10.1148/radiol.12111248>.
- Kitamoto E, Chikui T, Kawano S, Ohga M, Kobayashi K, Matsuo Y, et al. The application of dynamic contrast-enhanced MRI and diffusion-weighted MRI in patients with maxillofacial tumors[J]. *Acad Radiol.* 2015;22(2):210–6. <https://doi.org/10.1016/j.acra.2014.08.016>.
- Eissa L, Seif SA, Desooky SE, Eid M, Koraitim T. Accuracy assessment of combined diffusion weighed and dynamic gadolinium MR sequences in characterization of salivary gland tumors[J]. *Egypt J Radiol Nucl Med.* 2016;47:127–39. <https://doi.org/10.1016/j.ejmm.2015.11.011>.
- Takashima S, Noguchi Y, Okumura T, Aruga H, Kobayashi T. Dynamic MR imaging in the head and neck[J]. *Radiology.* 1993;189:813–21. <https://doi.org/10.1148/radiology.189.3.8234709>.
- Zheng SY, Xu ZF, Wu XH, Pan AZ. Use-fulness of dynamic contrast-enhanced MR imaging and diffusion weighted MR imaging for differentiation of benign and malignant parotid tumors[J]. *J Clin Med Imag.* 2018;1(1):1–6.
- Abdel Razek AAK, Samir S, Ashmalla GA. Characterization of parotid tumors with dynamic susceptibility contrast perfusion-weighted magnetic resonance imaging and diffusion-weighted MR imaging[J]. *J Comput Assist Tomogr.* 2017;41(1):131–6. <https://doi.org/10.1097/RCT.0000000000000486>.
- Yerli H, Agildere AM, Aydin E, Geyik E, Haberal N, Kaskati T, et al. Value of apparent diffusion coefficient calculation in the differential diagnosis of parotid gland tumors[J]. *Acta Radiol.* 2007;48(9):980–7. <https://doi.org/10.1080/02841850701501717>.
- Yuan Y, Tang W, Tao X. Parotid gland lesions: separate and combined diagnostic value of conventional MRI, diffusion-weighted imaging and dynamic contrast-enhanced MRI[J]. *Br J Radiol.* 2016;89(1060):20150912. <https://doi.org/10.1259/bjr.20150912>.
- Habermann CR, Arndt C, Graessner J, Diestel L, Petersen KU, Reitmeier F, et al. Diffusion-weighted echo-planar MR imaging of primary parotid gland tumors: is a prediction of different histologic subtypes possible?[J]. *AJNR Am J Neuroradiol.* 2009;30(3):591–6. <https://doi.org/10.3174/ajnr.A1412>.
- Assili S, Fathi Kazerooni A, Aghaghazvini L, Saligheh Rad HR, Pirayesh Islamian J. Dynamic contrast magnetic resonance imaging (DCE-MRI) and diffusion weighted MR imaging (DWI) for differentiation between benign and malignant salivary gland tumors[J]. *J Biomed Phys Eng.* 2015;5(4):157–68 eCollection 2015 Dec.
- Yabuuchi H, Matsuo Y, Kamitani T, Setoguchi T, Okafuji T, Soeda H, et al. Parotid gland tumors: can addition of diffusion-weighted MR imaging to dynamic contrast-enhanced MR imaging improve diagnostic accuracy in characterization?[J]. *Radiology.* 2008;249(3):909–16. <https://doi.org/10.1148/radiol.2493072045>.
- Li L, Wang K, Sun X, Wang K, Sun Y, Zhang G, et al. Parameters of dynamic contrast-enhanced MRI as imaging markers for angiogenesis and proliferation in human breast cancer [J]. *Med Sci Monit.* 2015;21:376–82. <https://doi.org/10.12659/MSM.892534>.
- Tofts PS, Brix G, Buckley DL, Evelhoch JL, Henderson E, Knopp MV, et al. Estimating kinetic parameters from dynamic contrast-enhanced t1-weighted MRI of a diffusable tracer: standardized quantities and symbols[J]. *JMRI.* 1999;10(3):223–32. [https://doi.org/10.1002/\(sici\)1522-2586\(199909\)10:3<223:aid-jmri2>3.0.co;2-s](https://doi.org/10.1002/(sici)1522-2586(199909)10:3<223:aid-jmri2>3.0.co;2-s).
- Ger R, Awan M, Mohamed A, Ding Y, Frank S, Howell R, et al. WE-FG-202-12: investigation of longitudinal salivary gland DCE-MRI changes[J]. *Med Phys.* 2016;43(6):3829. <https://doi.org/10.1118/1.4957924>.

Publisher's note Springer Nature remains neutral with regard to jurisdictional claims in published maps and institutional affiliations.